DOI: 10.21062/mft.2022.058 http://www.journalmt.com

Analysis of the Effect of Heat Treatment and Corrosion Load on the Microstructure and Microhardness of the Ti6Al4V Alloy

Iryna Hren (0000-0003-3942-2481), Sylvia Kuśmierczak (0000-0002-5135-4170), Roman Horký (0000-0002-4451-3006), Jaromír Mach
Faculty of Mechanical Engineering, J. E. Purkyne University in Usti nad Labem. Pasteurova 3334/7, 400 01 Usti nad Labem. Czech Republic. E-mail: sylvia.kusmierczak@ujep.cz, iryna.hren@ujep.cz

In terms of physical and chemical properties, titanium and its alloys are among the most important construction materials today. The Ti6Al4V alloy can be classified among high-strength materials with good plasticity, corrosion resistance and other valuable properties. When performing operations associated with long-term heating of workpieces and parts made of titanium alloys in an air atmosphere, a TiO_2 layer is formed on the surface of the product. Ti6Al4V alloy, also known as Ti64, in terms of microstructure is a two-phase alloy formed by α+β solid solutions, which has excellent corrosion resistance and biocompatibility. This alloy is also suitable for jet engines, gas turbines and many aircraft components, as well as in biomedicine. Heat treatment can further improve its technical properties, reduces stress, improves machinability, fracture toughness. The surface of alloys can also be thermally stressed when micro and nano layers of material are applied, which serve to extend the life of products made of this alloy. The presented article analyzes the effect of heat treatment at temperatures of 550 °C and 600 °C and corrosion load with salt fog in the range of 168 to 720 hours on the microstructure and microhardness of the Ti6Al4V alloy.

Keywords: Ti6Al4V alloy, corrosion, microhardness

1 Introduction

In terms of physical and chemical properties, titanium and its alloys are among the most important construction materials today. They are characterized by high strength, good plasticity, corrosion resistance exceeding that of stainless steels in seawater and a number of corrosive environments, and other valuable properties. Due to the polymorphism and martensitic transformation that occurs during accelerated cooling, a two-phase titanium alloy is formed, which can be effectively hardened by heat treatment. When heated, titanium and its alloys actively absorb gases – oxygen, nitrogen, hydrogen, creating gas-saturated layers with the structure of an interstitial solid solution. Inclusions of these compounds significantly increase the hardness and sharply reduce the impact strength and ability to plastic deformation [1]. When performing operations associated with long-term heating of workpieces and parts made of titanium alloys in an air atmosphere (such as hot deformation, heat treatment), a TiO_2 layer is formed on the surface of the product. For heat-deformed blanks, this layer does not exceed 50-70 microns [2]. Oxygen stabilizes the α-phase in titanium [1-3], which is why oxygen-saturated layers are called alpha-firing.

Ti6Al4V alloy, also known as Ti64, is an α+β (room temperature) titanium alloy with high strength, low density, excellent corrosion resistance and excellent biocompatibility [3,4]. The Ti6Al4V alloy was originally developed for aircraft structural applications in the 1950s. This light yet strong alloy is suitable for jet engines, gas turbines and many aircraft components [3-6].

Heat treatment of Ti6Al4V alloy for phase transformation can further improve its mechanical properties [5,6]. Heat treatment is used to remove metal stress, improve machinability, structural stability, fracture toughness, strength, etc. [7-8]. Manipulation of mechanical properties (microstructure, hardness, toughness, tensile strength) is achieved by heating the metal to the phase transition temperature. The cooling rate is another primary criterion for achieving microstructure control [9]. The transformation temperature β is key to the success of heat treatment of titanium alloys, this transition temperature can be derived using metallographic, electrical resistance, X-ray methods, etc. [10-12]. The experimental value of the β transition temperature of Ti6Al4V was determined as 995 °C [13]. The combination of annealing and aging is reported to provide grade 5 titanium alloy with a microstructure consisting of soft α at grain boundary β [14-15]. Various industries, especially the aerospace and automotive industries, have adopted several heat treatment methods in engineering to increase the strength of materials used in industry. Machine parts

in which Ti6Al4V are used are helicopter rotor blades, turbines, centrifugal pumps, etc. [16].

While the aerospace industry still dominates the demand for Ti6Al4V [17-20], other application areas in which these alloys are used are the automotive, energy, marine, chemical and biomedical industries. Low density, high strength, high corrosion resistance and biocompatibility are attractive properties of Ti6Al4V for applications such as bridges and implants [21-23]. Its applications have also been extended to the marine and chemical industries due to its high corrosion resistance to most corrosive acids and bases [23-25]. I confirm these results in my study by Klimas et al.[26] where they found that the action of Ringer's acid resulted in fragmentation of the structure and the formation of dendrites. These changes improved corrosion resistance and increased microhardness. There were no changes in the composition of the phases.

Despite the high demand, the production of Ti6Al4V products is always challenging due to their poor thermal conductivity [27], tendency to strain hardening [28], and active chemical reactivity to oxygen [29]. Conventional production of Ti6Al4V products consists of casting and rolling loose raw materials with subsequent processing into final shapes and dimensions. These traditional production processes always inevitably lead to a large amount of material waste, environmental burden, and high production costs and long delivery time [30,31]. In such circumstances, there is a need to analyze these alloys for the desired properties. The presented experiment is part of a larger research aimed at studying the reactions of the Ti6Al4V alloy structure to various loading methods.

2 Experimental material and methodology

For experimental purposes, 10 samples of the Ti-6Al-4V alloy were prepared, which were taken from a rolled rod with a diameter of 12 mm with the following chemical composition: Al-6.25 wt. %, C-0.08 wt.%, Fe-0.25 wt.%, V-4.01 wt.%, H-0.015 wt.%, N-0.05 wt.%, O-0.2 wt.%. It is the most widespread and most produced titanium alloy ever, which finds its application in all areas of human existence, from the aviation and space industry, through products of daily use, such as glasses, jewelry, watches, sports equipment, to body implants used in the field of biomedicine [32-34]. More than 50% of the world titanium production is represented by this alloy [35-37]. This alloy is easily hardenable, malleable and easily weldable in the presence of an inert gas or a vacuum. In addition, the alloy does not cause any reactions with body tissue in the human organism [38,39] and due to the protective coating of TiO_2, its high corrosion resistance is ensured [40-41].

The resulting samples had a cylindrical shape with the following parameters: length – 30 mm and diameter – 12 mm. Subsequently, 2 samples were left without any modifications and another 8 were subjected to a heat treatment process. Specifically, the samples were annealed at 550 °C and 600 °C for 2 hours. After that, the samples were left inside the oven until they were completely cooled. The next step was the corrosion load, which was carried out in accordance with the ČSN EN ISO 9227 standard [42]. The prepared samples were placed in the LIEBISCH corrosion chamber, where they were exposed to a salt fog environment consisting of a NaCl solution. The samples were left in the corrosion chamber for 168, 240, 480 and 720 hours, while the temperature was maintained at 35 °C throughout.

For the analysis of the microstructure of the layer and the base material, 10 samples were metallographically prepared - by wet grinding and then polishing with diamond emulsions from Struers. The last mechanical-chemical treatment was carried out using an Al2O3 suspension with a grain size of 0.3 μm. After subsequent etching with a mixture of nitric and hydrofluoric acids (Kroll etchant), the structures of the material were observed using light microscopy on a confocal laser microscope LEXT OLS 5000 from Olympus.

In the last step, the microhardness test of all samples was performed in accordance with the CSN EN ISO 6507-1 standard on the FUTURE-Tech FM-300 device [43]. A 136° diamond indenter creating a square impression was used to measure the microhardness. The load value determined HV 0.01 (F = 0.098 N, 10 g), which acted on the test specimen for 10 s. Due to the thickness of the layer, emphasis was placed on the selected diagonal of the indenter in order to respect the ISO 6507-1 standard.

3 Microscopic analysis

In the first stage, a microscopic analysis of a Ti-6Al-4V alloy sample (without heat treatment) was performed using an Olympus Lext 5000 laser microscope. Figure 1 characterizes the Ti-6Al-4V alloy without heat and corrosion stress (denoted as S0), for which typical equiaxed α+β structure. It is a two-phase structure, where the dark grains represent intercrystalline phases β, which are regularly and evenly arranged around the light grains of phase α. The individual grains are distributed without the slightest clusters of one or the other phase. The β-phase grains are smaller and irregular in shape compared to the α-phase grains, while the dark α-phase grains are larger and more regular in shape. As expected, the microstructure image of the S0 sample

showed a duplex microstructure containing α and β phases, due to the presence of vanadium, which in the alloy acts as a stabilizer of the β phase, and aluminum, which, on the other hand, stabilizes the α phase.

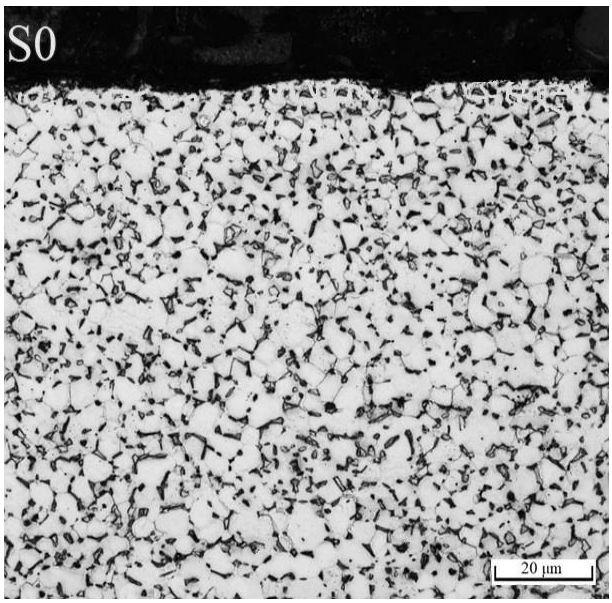

Fig. 1 *Microstructure of reference sample S0*

4 Microscopic analysis of samples after heat treatment and corrosion loading

As already mentioned in the theoretical part, heat treatment increases both the mechanical properties of the material and its resistance to corrosion. From a number of professional articles [32-40], which deal with the formation of a surface oxide layer as a result of thermal oxidation, it can be read that its gradual growth can already be observed from 500 °C. At lower processing temperatures, as a rule, lower thicknesses are achieved, but higher compactness and better adhesion. Higher temperatures (600 °C and more) can ensure the formation of a stronger surface layer, which provides higher values of selected mechanical properties, but if the conditions of the entire process are chosen incorrectly, there is a risk of worse adhesion of this mainly crystalline layer. In the aforementioned experiment, temperatures from lower ranges are presented, for the reason that this heat treatment is less energy-intensive, which is a current topic in particular today. The results for individual temperatures are presented in the following chapters.

Heat treatment of the resulting sample was carried out in an electric resistance furnace at a temperature of 550 °C and then 600 °C for 2 hours. By simply visual observation of the heat-treated samples (see Fig. 2), quite significant surface discoloration was detected. The color changed from the original light gray-blue to dark gray to brown as the temperature increased from 550 °C to 600 °C (samples are labeled SI and SII).

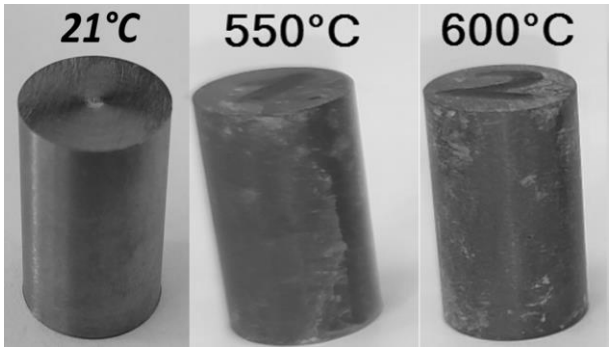

Fig. 2 *Coloration of heat-treated samples*

After that, the samples were left in the corrosion chamber for 168, 240, 480 and 720 hours (samples SI1, SI2, SI3, SI4 and then SII1, SII, SII3, SII4), while the temperature was maintained at 35 °C the whole time. The corrosion test was performed in accordance with the ČSN EN ISO 9227 standard [43]. Subsequently, the samples were cleaned of corrosion products, dried and cut, from which metallographic cuttings were subsequently prepared (in the same way as in the previous chapter), which were subsequently subjected to microscopic analysis.

Metallographic images of the microstructure of thermally oxidized and corrosion-stressed samples are shown in Fig. 3 and 4. Looking at the images of samples SI4 to SII4, it is evident that no structural changes occurred from the point of view of the base material. All the mentioned samples, like the S0 sample, consist of a fine-grained structure with a regular and uniform distribution of the grains of both phases.

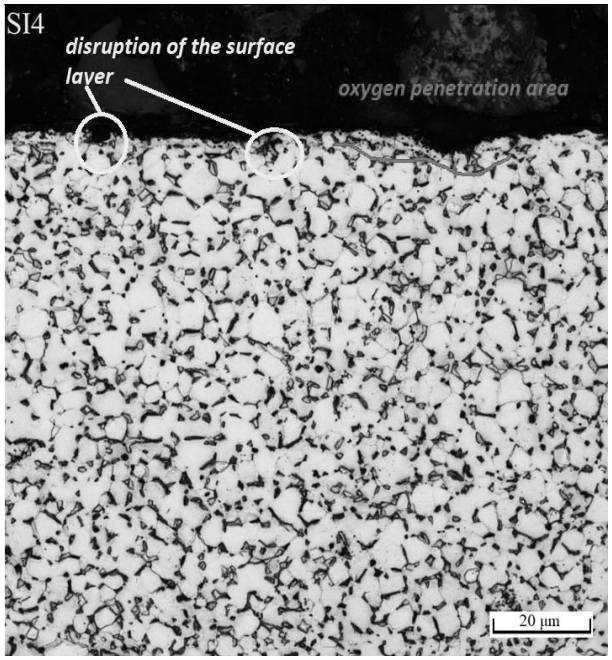

Fig. 3 *Microstructure of the Ti6Al4V after heat theatment (550 °C) and maximum corrosion load (720 hours)*

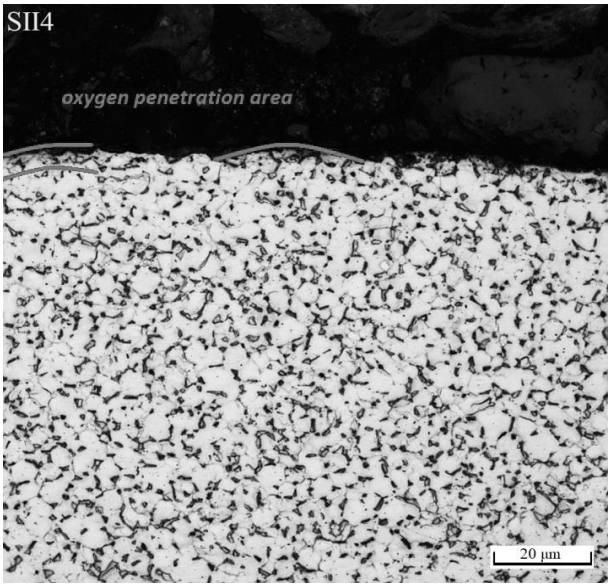

Fig. 4 *Microstructure of the Ti6Al4V after heat theatment (600 °C) and maximum corrosion load (720 hours)*

On the other hand, a TiO_2 layer was formed in both samples (The CO_2 layers were analyzed and checked by electron microscopy using EDX analysis. However, the more detailed results of these analyzes are not part of the presented article.). The only difference observed in the sample after corrosion loading for 720 h was that a more stable TiO_2 layer was observed in the SII4 sample.

5 Evaluation of microhardness

The microhardness of all samples was measured according to the ČSN EN ISO 6507-1 standard [44]. The research was carried out on a FUTURE-Tech FM-300 device. A 136° square indentation diamond indenter was used to measure microhardness, and the load value determined HV 0.01 (F = 0.098 N, 10 g). The duration of the load, which acted on the test body, was determined to be 10 s. The microhardness values of the reference sample S0, i.e. the sample without any heat treatment and corrosion load, are given in Tab. 1.

Tab. 1 *Microhardness values of reference sample S0*

S0 – HV0.01							
distance [µm]	10	25	50	75	100	125	150
Ø value	305.1	302.3	305.5	304.0	305.3	307.5	305.2
standard deviation	3.9	1.8	1.7	3.1	0.8	1.1	2.5

Tables 2 and 3 below show the measured microhardness values of the SI sample set. In Tab. 2 shows the values of the heat-treated SI0 sample, which was not subject to corrosion. In Tab. 3 shows the values of the samples that were first heat-treated under the same conditions and then subjected to a corrosion load.

Tab. 2 *Microhardness values of sample SI0*

SI0 – HV0.01							
distance [µm]	10	25	50	75	100	125	150
Ø value	345.5	337.5	334.5	337.5	333.5	340.5	338.0
standard deviation	3.5	2.5	0.5	5.5	7.5	3.5	3.0

The increase in hardness is caused by the breakdown of the martensitic structure, i.e., $\alpha' \rightarrow \alpha + \beta$. This happens because the martensite structure is not formed after heat treatment, the hardness increases during the aging process probably due to the precipitation of the fine α phase from the β phase, i.e., metastable $\beta \rightarrow$ fine $\alpha + \beta$ [45]. The heat-treated structure showed microhardness values of around 350 HV compared to the untreated one, which set - 300 HV.

Tab. 3 *Microhardness values of reference samples SI1-SI4*

SI1 – HV0.01							
distance [µm]	10	25	50	75	100	125	150
Ø value	360.2	345.0	338.9	333.9	328.0	321.5	314.8
standard deviation	10.4	2.8	2.1	2.4	3.4	4.7	3.5
SI2 – HV0.01							
distance [µm]	10	25	50	75	100	125	150
Ø value	366.5	327.4	324.9	327.3	326.7	332.6	324.7
standard deviation	2.7	2.9	4.3	7.8	3.5	4.6	3.6
SI3 – HV0.01							
distance [µm]	10	25	50	75	100	125	150
Ø value	378.7	362.7	356.4	347.2	345.2	340.4	337.7
standard deviation	4.7	3.9	3.2	5.6	6.1	5.0	3.5
SI4 – HV0.01							
distance [µm]	10	25	50	75	100	125	150
Ø value	375.3	358.6	354.5	347.1	342.3	338.6	336.8
standard deviation	5.5	3.0	4.3	7.7	7.7	6.4	7.1

From the above-mentioned Table 3, i.e. from the summary Fig. 5, which is presented below, it is possible to confirm the stated results from the previous chapter for this variant. Heat treatment at 550 °C resulted in the formation of an oxide layer, which caused an approximately 15% increase in hardness in the area just below the surface (10 μm) and an approximately 10% increase in the base material area compared to the S0 reference sample. As can be seen further, as a result of the corrosion action, corrosion products began to form on the surface, which by their nature caused a further increase in hardness in close proximity to the surface. Here, a gradual increase can be seen depending on the length of the corrosion load, with the highest values being achieved for the SI3 specimen. For sample SI4, a decrease has already occurred due to damage and separation of the surface layer due to corrosion attack.

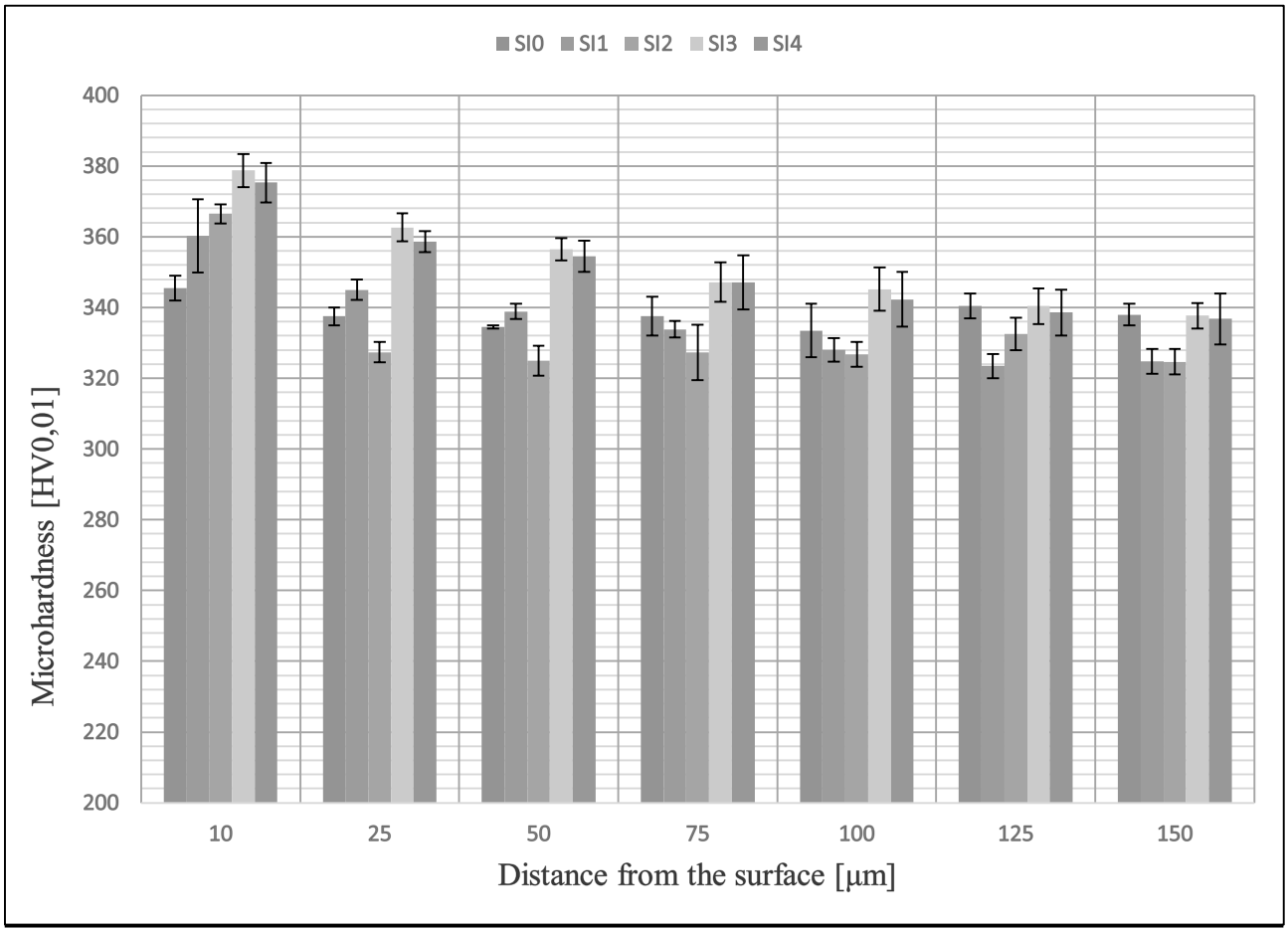

Fig. 5 *Diagram of average microhardness values of the SI sample set*

The measured values of the microhardness of only heat-treated samples are given in Tab. 4, values of heat treated and corrosion loaded in Tab. 5. A summary comparison of these samples can then be seen in Fig. 6.

Tab. 4 *Microhardness values of sample SII0*

SII0 – HV0.01							
distance [μm]	10	25	50	75	100	125	150
Ø value	344.0	349.5	349.5	349.5	352.0	345.0	347.0
standard deviation	1.0	2.5	0.5	4.5	1.0	3.0	2.0

In the case of sample SII0, which was heat treated at 600 °C and was not subjected to corrosion loading, there were very similar results to those obtained with variant SI. In this case too, the hardness increased by approximately 40 HV. Only with the difference that the difference of approximately 10 HV in microhardness between the surface and the base material was no longer detected. Practically the same average values were achieved in the entire measured cross-section. The maximum standard deviation reached a value of 4.5. These results also confirm the statement from the previous chapter, namely that a comparable thickness of the surface layer with the SI sample was achieved, which also corresponds to the resulting microhardness values.

Tab. 5 *Microhardness values of samples SII1-SII4*

SII1 – HV0.01							
distance [µm]	10	25	50	75	100	125	150
Ø value	388.0	376.6	368.2	359.5	353.9	346.3	342.3
standard deviation	4.1	6.5	8.9	7.4	8.2	9.0	6.0
SII2 – HV0.01							
distance [µm]	10	25	50	75	100	125	150
Ø value	386.3	374.9	365.3	352.5	348.6	343.2	338.8
standard deviation	3.6	3.8	6.1	5.8	5.3	5.6	5.5
SII3 – HV0.01							
distance [µm]	10	25	50	75	100	125	150
Ø value	380.2	371.7	365.7	358.2	351.8	347.2	342.6
standard deviation	4.7	2.2	2.9	6.0	5.9	5.8	5.7
SII4 – HV0.01							
distance [µm]	10	25	50	75	100	125	150
Ø value	383.1	376.2	371.5	366.3	361.3	356.4	352.3
standard deviation	4.9	3.1	2.4	2.3	2.3	2.3	2.0

From the measured microhardness results, shown in Tab. 6 and visualized in Fig. 6, the effect of the heat treatment on the hardness of the layer affected by the heat treatment and the corrosion load is already becoming apparent. After this set was subjected to corrosion loading, all samples showed an increase in microhardness of approximately 40 HV within 10 µm from the surface, with increases visible down to a depth of approximately 50 µm from the surface. As a result of the presence of a corrosive environment, corrosion by-products were formed, which were manifested externally by an additional increase in microhardness. A similar phenomenon was also observed in the work of Kumar [46], where a maximum value of 420 HV was reached. The formation of corrosion products occurred during the first stage of corrosion loading, which affected the corrosion behavior by preventing further exposure to the environment. For this reason, at a distance of 10 µm, no difference is observed between samples SII1 and SII4, i.e. samples subjected to corrosion for 168 and 720 hours.

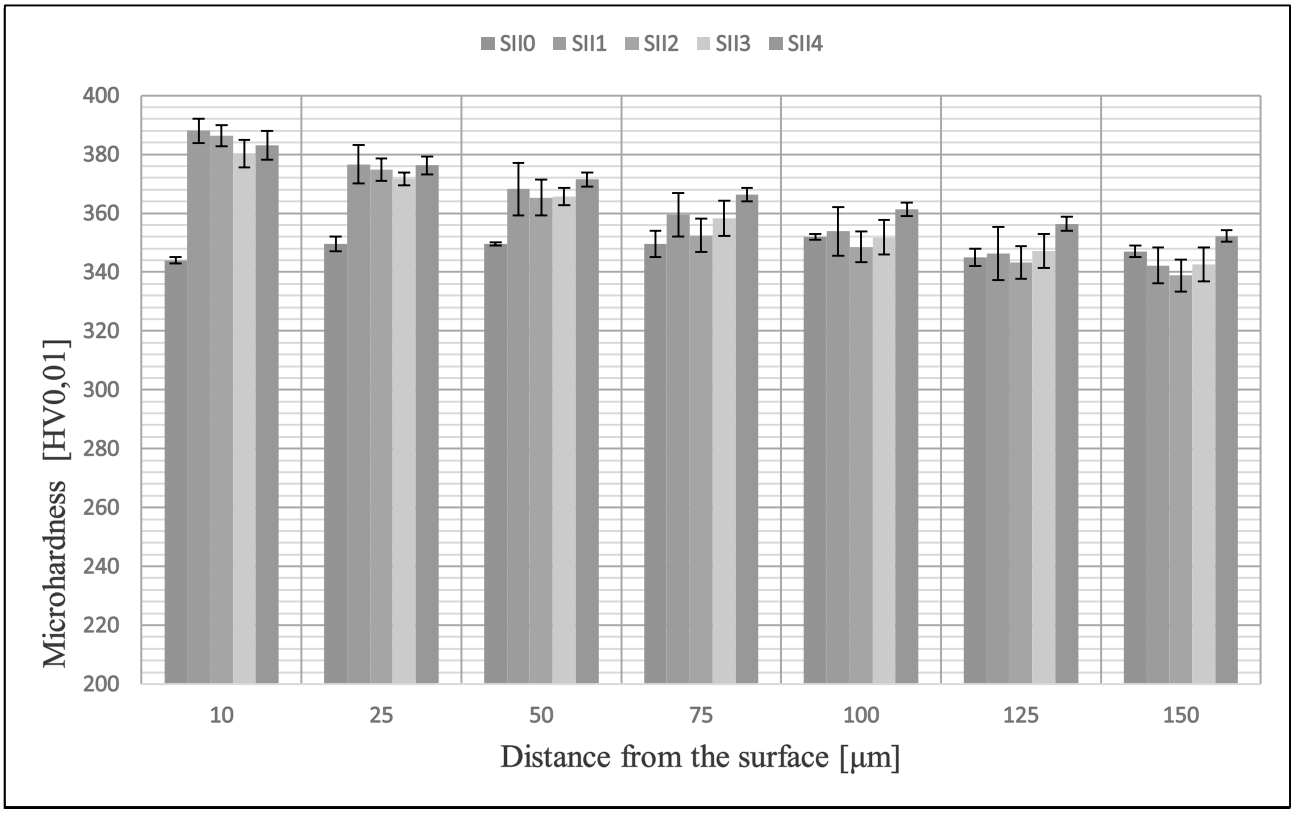

Fig. 6 *Diagram of average microhardness values of a set of SII samples*

6 Conclusion

The presented article deals with the effect of heat treatment on selected properties of the Ti6Al4V alloy. During the experiment, two different heat treatment temperatures were used: 550 °C and 600 °C with cooling in a closed furnace. These samples were compared with non-heat treated samples. After that, the samples were subjected to a corrosion load for 168 to 720 hours.

The microstructure of the resulting samples did not show any striking differences. The only difference was the formation of compact TiO_2 layers. This phenomenon confirmed our expectations and we can focus on higher temperatures during heat treatment in the next work.

Higher temperatures (annealing process) cause an increase in microhardness. Samples treated at 550 °C reached a microhardness value of approx. 336 HV and samples treated at 600 °C – approx. 350 HV. Hardness increases during aging probably due to precipitation of fine α phase from β phase, i.e., metastable $\beta \rightarrow$ fine $\alpha + \beta$. Which will also be the interest of further research.

From the point of view of the performed experiment, it can be assumed that a further increase in temperature during heat treatment will cause an increase in both microhardness and other mechanical properties (strength, hardness, etc.). Therefore, further research will be focused on investigating the microstructure, mechanical and corrosion properties of this alloy depending on heat treatment under other conditions.

Acknowledgement

Supported by the project SGS UJEP-SGS-2020-48-002-2.

References

[1] PRYMAK, O., BOGDANSKI, D., KÖLLER, M., ESENWEIN, S., & col. (2005). Morphological characterization and in vitro biocompatibility of a porous nickel–titanium alloy. *Biomaterials,* Vol. 26, Issue 29, pp. 5801-5807. ISSN 0142-9612

[2] BROOKSHIRE, F. V. G., NAGY, W. W., DHURU, V. B., ZIEBERT, G. J., CHADA, S. (1997). The qualitative effects of various types of hygiene instrumentation on commercially pure titanium and titanium alloy implant abutments: an in vitro and scanning electron microscope study

[3] LEYENS, C., PETERS, M. (2003). Titanium and titanium alloys, Fundamental and applications. *WILEY-VCH*, pp. 333-350, 401-404. ISBN:9783527602117

[4] XIAOGUANG, F., QI, L., ANMING, Z., YUGUO, S., WENJIA M. (2017). The Effect of Initial Structure on Phase Transformation in Continuous Heating of a TA15 Titanium Alloy. *Metals*, Vol. 7, No. 6, pp. 1-12. ISSN 2075-4701

[5] PEDERSON, R., BABUSHKIN O., SKYSTEDT F. AND WARREN R. (2003). Use of High Temperature X-ray Diffractometry to Study Phase Transitions and Thermal Expansion Properties in Ti – 6Al – 4V. *Materials Science and Technology*, Vol.19, No. 11, pp. 1533-1538.

[6] LEE, K., YANG, S., YANG, J. (2017) Optimization of Heat-treatment Parameters in Hardening of Titanium Alloy Ti-6Al-4V by using the Taguchi Method. *International Journal of Advanced Manufacturing and Technology*, Vol. 90, pp. 753-761.

[7] HUA, Q., WEIDONG, L. (2011) Theoretical Calculation of β Transition Temperature of Ti-6Al-4V from Valence Electron Level. *Advanced Materials Research,* pp. 299-300, ISSN: 1662-8985

[8] FIDAN, S., AVCU, E., KARAKULAK, E., YAMANOGLU, R., ZEREN M., SINMAZCELIK T. (2013). Effect of Heat Treatment on Erosive Wear Behaviour of Ti6Al4V alloy. *Materials Science and Technology,* Vol. 29, No. 9, pp. 1088-1094

[9] Imam, M. A., Gilmore, C. M., (1983) Fatigue and Microstructural Properties of Quenched Ti-6AI-4V. *Metallurgical Transactions A,* Vol. 14, pp. 223-240

[10] SUDHAGARA, R. S., JITHIN, V., GEETHA, M., NAGESWARA R. M. (2018). Processing of Beta Titanium Alloys for Aerospace and Biomedical Applications. *Titanium Alloys – Novel Aspects of Their Manufacturing and Processing Intech,* Open 1-18

[11] HADKE, S., KHATIRKAR, R. K., SHEKHAWAT, S. K., JAIN, S., SAPATE, S. G. (2015) Microstructure Evolution and Abrasive Wear Behavior of Ti-6Al-4V Alloy. *Journal of Materials Engineering and Performance,* Vol. 24, pp. 3969-3981

[12] SEMIATIN, S. L., KNISLEY, S. L., FAGIN, P. N., ZHANG, F., BARKER D. R. (2003). Microstructure Evolution during Alpha-Beta Heat Treatment of Ti-6Al-4V. *Metallurgical and Materials Transactions A,* Vol. 34, pp. 2377-2386

[13] QU, S. G., SUN, F. J., YUAN, Z. M., LI, G., LI Q. (2015). Effect of Annealing Treatment on Microstructure and Mechanical Properties of Hot Isostatic Pressing Compacts Fabricated using Ti–6Al–4V Powder. *Powder Metallurgy*, Vol. 58, No. 4, pp. 312-319

[14] JOVANOVIC, M. T., TADIĆ, S., ZEC S., MIŠKOVIC, Z., BOBIĆ I. (2006). The Effect of Annealing Temperatures and Cooling Rates on Microstructure and Mechanical Properties of Investment Cast Ti–6Al–4V Alloy. *Materials and Design*, Vol. 27, No. 3, pp. 192-199. ISSN 0261-3069

[15] RAJAGOPAL, K. P. A., JOSE, A. M., SOMAN, A., DCRUZ, C. J., NIVED, S. N., SYAMRAJ, S., VIMALKUMAR P. (2015). Investigation of Physical and Mechanical Properties of Ti Alloy (Ti-6Al-4V) Under Precisely Controlled Heat Treatment Processes. *International Journal of Mechanical Engineering and Technology,* Vol. 6, No. 2, pp. 116-127. ISSN 0976 – 6359

[16] KLIMAS, J., SZOTA, M., NABIAŁEK, M., ŁUKASZEWICZ, A., BUKOWSKA, A. (2013). Comparative description of structure and properties of Ti6Al4V titanium alloy for biome dical applications produced by two methods: conventional (molding) and innovative (injection) ones, *Journal of Achievements in Materials and Manufacturing Engineering*. Vol. 61, No. 2, pp. 195-201

[17] FOMIN, F., FROEND, M., VENTZKE, V., ALVAREZ, P., BAUER, S., KASHAEV, N. (2018). Metallurgical aspects of joining commercially pure titanium to Ti-6Al-4V alloy in a T-joint configuration by laser beam welding. *The International Journal of Advanced Manufacturing Technology*, Vol. 97, pp. 2019–2031

[18] LIU, S., SHIN, Y. C. (2019). Additive manufacturing of Ti6Al4V alloy. *Materials & Design*, Vol.164, 107552, ISSN 0264-1275

[19] HÖNNIGE, J.R., COLEGROVE, P. A., AHMAD, B., FITZPATRICK, M. E., GANGULY, S., LEE, T. L., WILLIAMS, S. W. (2018). Residual stress and texture control in Ti-6Al-4V wire + arc additively manufactured intersections by stress relief and rolling, pp. 193-205. *Mater. Des.*, 150

[20] HAYES, B.J., MARTIN, B. W., WELK, B., KUHR, S. J., ALES, T. K., BRICE, D. A., GHAMARIAN, I., BAKER, A.H., HADEN, C. V., HARLOW, D. G., FRASER, H. L., COLLINS P. C. (2017). Predicting tensile properties of Ti–6Al-4V produced via directed energy deposition, *Acta Mater*. Vol. 133, pp. 120-133. ISSN 1359-6454

[21] NIINOMI, M. (2003). Recent Research and Development in Titanium Alloys for Biomedical Applications and Healthcare Goods. *Science and Technology of Advanced Materials,* Vol. 4, No. 5, pp. 445-454. ISSN 1468-6996

[22] CHEN, J., PAN, C. (2011). Welding of Ti-6Al-4V alloy using dynami- cally controlled plasma arc welding process. *Transactions of Nonferrous Metals Society of China,* Vol. 21, No. 7, pp. 1506–1512. ISSN 1003-6326

[23] WU, M., XIN, R., WANG, Y., ZHOU, Y., WANG, K., LIU Q. (2016). Microstructure, texture and mechanical properties of commercial high-purity thick titanium plates jointed by electron beam welding. *Materials Science and Engineering,* Vol. 677, pp. 50–57

[24] SQUILLACE, A., PRISCO, U., CILIBERTO, S., ASTARITA, A. (2012). Effect of welding parameters on morphology and mechanical properties of Ti-6Al-4V laser beam welded butt joints. *Journal of Materials Processing Technology*, Vol. 212, pp. 427–436. ISSN 0924-0136

[25] KASHAEV, N., VENTZKE, V., FOMICHEV, V., FOMIN, F., RIEKEHR. S. (2016). Effect of Nd:YAG laser beam welding on weld morphology and mechanical properties of Ti–6Al–4V butt joints and T-joints. *Optics and Lasers in Engineering,* Vol. 86, pp.172–180

[26] LI, X., XIE, J., ZHOU, Y. (2005). Effect of oxygen contamination in the argon shielding gas in laser welding of commercially pure titanium thin sheet. *J Mater Sci,* Vol. 40, pp. 3437–3443

[27] DAI, N., ZHANG, L. C., ZHANG, J., CHEN, Q., WU, M. (2016). Corrosion behavior of selective laser melted Ti-6Al-4 V alloy in NaCl solution. *Corros. Sci.,* Vol. 102, pp. 484-489

[28] BAI, Y., GAI, X., LI, S., ZHANG, L. C., LIU, Y., HAO, Y., ZHANG, X., YANG, R., GAO, Y. Improved corrosion behaviour of electron beam melted Ti-6Al–4V alloy in phosphate buffered saline. *Corrosion Science,* Vol. 123, pp 289-296. ISSN 0010-938X

[29] ZIELIŃSKI, A., SOBIESZCZYK, S. (2010). Corrosion of Titanium Biomaterials, Mechanisms, Effects and Modelisation. *Corrosion Reviews*, Vol. 26, pp 1-22

[30] KOUŘIL, M. (2011). Corrosion rate of construction materials in hot phosphoric acid

with the contribution of anodic polarization. Weinheim. *Materials and Corrosion*, Vol. 63, No. 4, pp. 310-316

[31] KRYSHNA, D. S. R. (2006). Thick rutile layer on titanium for tribological applications. *Tribology International*, Vol. 40, No. 2, pp 329-334. Singapore. ISSN 0301-679X

[32] LIU, S., SHIN, Y. C. (2019) Additive manufacturing of Ti6Al4V alloy. *A review, Materials & Design*, Vol. 164, ISSN 0264-1275

[33] VASILKO, K. (2019). Titanium and Technological Problems of Its Machining. *Manufacturing Technology*, Vol. 19, No. 3, pp. 525-530. ISSN 1213–248

[34] HANUSOVÁ P., PALČEK P., UHRÍČIK M. (2019). Analysis of the Cause of Titanium Endoprosthesis Failure. *Manufacturing Technology*, Vol. 19, No. 5, pp. 749-752

[35] UHLMANN, E., KERSTING, R., KLEIN, T. B., CRUZ, M. F., BORILLE. A. V. (2015). Additive manufacturing of titanium alloy for aircraft components. *Proc. CIRP*, Vol. 35, pp. 55-60. ISSN 2212-8271

[36] EMMELMANN, C., SANDER, P., KRANZ, J., WYCISK, E. (2011). Laser additive manufacturing and bionics: redefining lightweight design. *Phys. Procedia*, Vol. 12, pp. 364-368. ISSN 1875-3892

[37] HAO, Y. L., LI, S. J., YANG, R. (2016). Biomedical titanium alloys and their additive manufacturing. *Rare Metals*, Vol. 35, No. 9, pp. 661-671

[38] GIANNATSIS, J., DEDOUSSIS V. (2009). Additive fabrication technologies applied to medicine and health care. *Int. J. Adv. Manuf. Technol.,* Vol. 40, No. 1, pp. 116-127

[39] MARTIKAN, A., STRUHARNANSKY, J., STANCEKOVA, D., CZAN, A., HATALA, M. (2015). Influence of Chemical Etching on Surface Micro-Geometry of Titanium Implants. *Manufacturing Technology, Vol.* 15, No. 4, pp. 601-604

[40] STANCEKOVA, D., SEMCER, J., RUDAWSKA, A., CEP, R. (2015). Identification of Drilling of Biocompatible Materials Based on Titanium. *Manufacturing Technology*, Vol. 15, No. 4, pp. 699-704

[41] GORYNIN, I. V. (1999). Titanium alloys for marine application. *Materials Science and Engineering: A*, Vol. 263, No. 2, pp. 112-116. ISSN 0921-5093

[42] ORYSHCHENKO, A. S., GORYNIN, I. V., LEONOV, V. P., KUDRYAVTSEV, A. S., MIKHAILOV, V. I., CHUDAKOV E.V. (2015) Marine titanium alloys: present and future. *Inorg. Mater. Appl. Res.*, Vol. 6, No. 6, pp. 571-579

[43] ČSN EN ISO 9227 (038132). Corrosion tests in artificial atmospheres - Salt spray tests. ISO 9227:2017

[44] ČSN EN ISO 6507-1 (420374). Metallic materials - Vickers hardness test - Part 1: Test method. ISO 6507-1:2018

[45] BAHRAMINASAB, M., SAHARI, B. B., EDWARDS, K. L., FARAHMAND, F., ARUMUGAM, M., HONG, T. S. Aseptic loosening of femoral components – A review of current and future trends in materials used. *Materials & Design*, Vol. 42, pp. 459-470

[46] KUMAR, S., (2010) Thermal oxidation of Ti6Al4V alloy: Microstructural and electrochemical characterization. *Materials Chemistry and Physics,* Vol. 119, pp. 337-346. ISSN 0254-0584